



ORIGINAL PAPER

MULTI-ANNUAL MASS VARIATIONS FROM GRACE MONTHLY SOLUTIONS –
PRELIMINARY RESULTSAnnamária KISS ^{1)*} and Lóránt FÖLDVÁRY ^{2,3)}

1) Department of Geodesy and Surveying, Budapest University of Technology and Economics,
Muegyetem rkp 3 KM 26, H-1111 Budapest, Hungary

2) Institute of Geoinformatics, Alba Regia Technical Faculty, Óbuda University, Budai út 45., 8000 Székesfehérvár, Hungary

3) Geodetic and Geophysical Institute, Research Centre of Astronomical and Earth Sciences, Hungarian Academy of Science, Csatkai Endre
u. 6-8, 9400 Sopron, Hungary

*Corresponding author's e-mail kiss.annamaria@epito.bme.hu

ARTICLE INFO

Article history:

Received 18 February 2018

Accepted 29 May 2018

Available online 8 June 2018

Keywords:

GRACE
Multi-annual mass variations
Hydrology
Gravity

ABSTRACT

The GRACE satellites have provided gravity field solutions with approximately monthly resolution since April 2002. The monthly solutions enable investigations of the annual, semi-annual and secular mass variations, which mainly occur in a thin layer of the Earth's surface. By the end of the GRACE science mission in 2017, the time span has increased to 15 years, making the possibility of determining longer-period variations feasible. First attempts to determine multi-annual variations, i.e. periods of some years but less than 10, are presented in this study. A combination of 3 different PSD estimation methods has been used for identifying the regions of multi-annual mass variations. As a result, 8 different areas have been found with significant multi-annual mass variations. The source of multi-annual mass variations in most detected regions can be identified as related to the ENSO cycle.

1. INTRODUCTION

The GRACE (Gravity Recovery And Climate Experiment) twin satellites have been providing measurements of the Earth's gravity field since their launch in 2002 (Tapley et al., 2004). Mapping the gravity field requires accurate measurements of the varying distance between the two satellites via microwave ranging system, while the precise positions of the satellites are recorded using GPS tracking, and the non-gravitational effects are detected by measurements of on-board accelerometers. Based on these measurements, processing centres produce different levels of GRACE data, which have been the basis of numerous studies targeting the analysis of the time-varying gravity field. These variations occur mainly due to mass redistributions near the surface of the Earth, thus GRACE data have been used to analyse major mass variations and their effect on the gravity field. Annual and semi-annual periodic gravity field variations have been studied widely, as well as secular trends (JPL, 2018). With nearly 15 years of data available, it has become feasible to apply GRACE data to observe multi-annual periodic signals. In this study, spectral analysis of the time series has been performed in order to detect multi-annual variations with periods between 3 and 7 years.

Silverii et al. (2016) has observed 2.5-yearly periodicity of transient deformation of karst aquifers due to hydrology has been detected both from GPS and GRACE. Their study has made use of GRC Tellus Land solutions (c.f. Swenson, 2012). This solution is

generally similar to our solutions, applying also a 300 km Gaussian smoothing filtering, and probably a similar de-stripping method. According to our experience, to derive information on 2.5-year period is possible but challenging due its spectral closeness to the annual frequency. Thus our study focuses rather on the 3-7 year periodic variations.

The connection between El Niño-Southern Oscillation (ENSO) and the global air temperature (GAT) is studied by Privalsky and Jensen (1994). According to their analysis, the ENSO contributes more energy to variations of GAT at large and intermediate, i.e. 4-6 years, time scales. This is exactly that periods, which can be determined (and is determined in this study) from the available GRACE data. Considering that air temperature variations generate variation of density, which manifests in the form of mass redistribution, the contribution of ENSO to the GAT may also be traced by changes of the gravity field. Therefore, link between multi-annual variations and ENSO is presumable, and will be analysed in this study.

However, the determination of multi-annual variations is methodologically critical. Basically, energy content of any signal can be investigated by determining the Power Spectral Density (PSD), which defines how the power of the signal is distributed over frequency. The derivation of PSD is however method dependent. The aim of this study is basically to detect whether any multi-annual mass variation can be detected in the GRACE mass anomaly series, and then

to interpret it. The study is constructed accordingly: after a brief overview of the used data and the derivation of mass anomaly time series, methodology of PSD determination is discussed. Using 3 methods for PSD determinations, a method is developed for detecting probable locations of multi-annual variations. Subsequently, the regions with probable multi-annual mass variations are then analysed, and the source of the variation is interpreted.

2. TIME SERIES ANALYSIS IN THE FREQUENCY DOMAIN

The computed surface mass anomaly time series represent temporal mass variations of a point at any arbitrary location defined by ϕ , λ and r . In this study, mass anomaly time series have been analysed in the frequency domain in order to search for variations with longer periodicities. PSD estimations have been used to discover substantial, however less conspicuous periodicities of the surface mass anomaly time series.

A basic way to estimate the PSD of an L -length signal (x_n) is to compute the discrete-time Fourier transform and scale the squared magnitude:

$$P_x(f) = \frac{1}{L} \left| \sum_{n=1}^L x_n e^{-2\pi i f t_n} \right|^2 = \frac{1}{L} \left[\left(\sum_n x_n \cos 2\pi f t_n \right)^2 + \left(\sum_n x_n \sin 2\pi f t_n \right)^2 \right] \quad (1)$$

This method is called the periodogram. The periodogram is not a consistent estimator of the PSD, since its variance does not decrease as the L length of the time series increases. There have been numerous techniques created to improve the variance of the estimation.

Welch (1967) proposed a method of dividing the time series into overlapping segments then computing modified periodograms by convolving it with a Hamming window and averaging the results. Computing PSD from shorter data leads to reduced resolution, although the averaging of more estimates successfully decreases the variance. An optimal trade-off between higher resolution and lower variance can be achieved by modifying the window size.

Thomson (1982) described a multitaper method. After windowing the time series with multiple orthogonal windows (tapers), the averaging of the PSD estimations gives an improved result. The optimal choice of the number of tapers leads to decreased variance, bias and spectral leakage.

All methods mentioned above require data with a constant sampling frequency. However, time series from GRACE measurements are not uniformly sampled. Creating a new time vector with equal spacing and using any kind of interpolation leads to slightly modified surface mass anomaly time series deforming the spectral characteristics.

An alternate option to estimate PSD based on non-uniformly sampled time series, is the Lomb-Scargle periodogram, developed by Lomb (1976) and refined by Scargle (1982):

$$P_x(t) = \frac{1}{2} \left\{ \frac{\left[\sum_n x_n \cos 2\pi f (t_n - \tau) \right]^2}{\sum_n \cos^2 2\pi f (t_n - \tau)} + \frac{\left[\sum_n x_n \sin 2\pi f (t_n - \tau) \right]^2}{\sum_n \sin^2 2\pi f (t_n - \tau)} \right\} \quad (2)$$

where the time-offset τ is specified for each f :

$$\tau = \frac{1}{4\pi f} \arctan \frac{\sum_n \sin 4\pi f t_n}{\sum_n \cos 4\pi f t_n} \quad (3)$$

A special feature of the Lomb-Scargle periodogram is that the value of P_x at a given frequency is identical to the result of a least-squares fitting of a sinusoid with the same frequency:

$$y(t) = A \cos 2\pi f t + B \sin 2\pi f t \quad (4)$$

In this study, the Welch's, Thomson's and Lomb-Scargle's methods have been used to estimate the PSD of the time series (CSR, GFZ and JPL as well) in the following manner (based on empirical tests):

- In case of Welch's method, the interpolated time series have been divided into 5 segments with 50 % overlap. Each segment has been windowed with a Hamming window and a periodogram has been computed at 241 frequencies. The result is the average of the 5 periodograms at each $1^\circ \times 1^\circ$ grid points.
- Thomson's multitaper method has been used to estimate the PSD from the interpolated time series as well. Four different Slepian's tapers have been used and the results have been averaged.
- The Lomb-Scargle's periodogram has been used to estimate the PSD based on the original unevenly sampled time series at the same 241 frequencies.

To identify the areas with significant multi-annual periodicities, high PSD values have been searched at frequencies corresponding to periods between 3 and 7 years.

3. DATA AND PROCESSING

The Level-1B, Level-2 and Level-3 products derived from the measurements of the GRACE satellites have been made public to support various scientific studies. The Level-1B products include several datasets (inter-satellite range, range-rate, range-acceleration, non-gravitational acceleration from each satellite, etc.) calculated from the raw observations. Apart from AOD products, which have been produced by the German GeoForschungs-Zentrum (GFZ), all other Level-1B products are coded and operated by the Jet Propulsion Laboratory of NASA (JPL). The Level-2 products consist of monthly sets of spherical harmonics calculated from the Level-1B products, and have been made available by three official processing centres, the Center of Space Research, University of Texas (CSR), the GFZ and JPL. The Level-3 products contain value-added products (e.g., maps and time series) which are

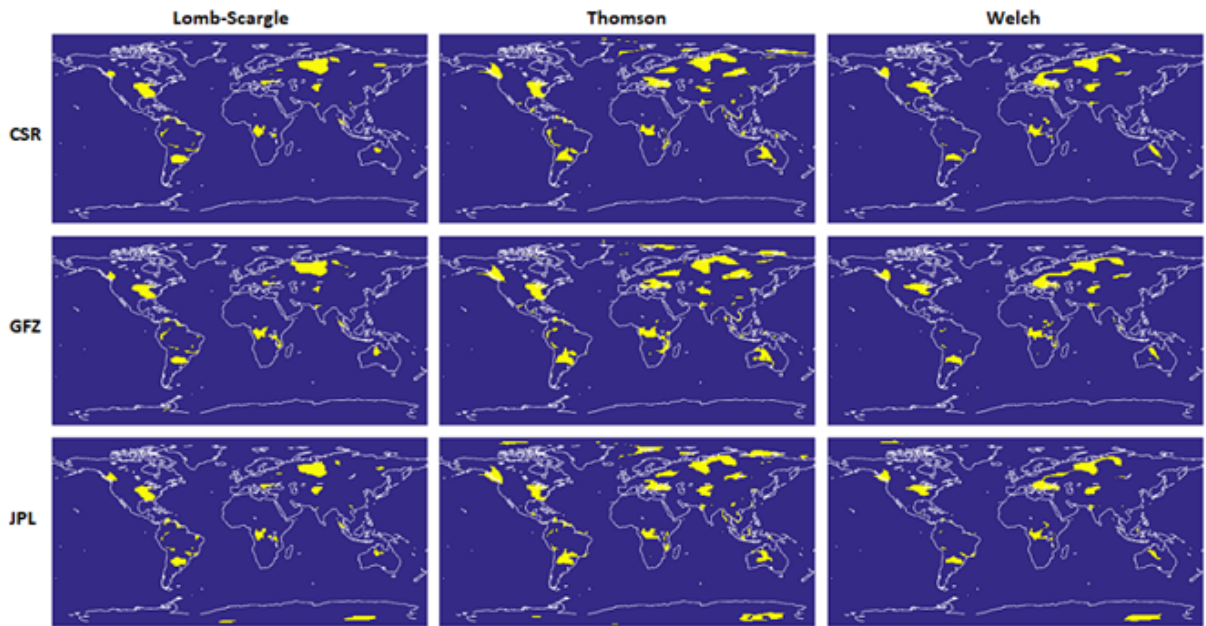


Fig. 1 Comparison of results based on the CSR, GFZ and JPL GRACE data and computed with the methods of Lomb-Scargle, Thomson and Welch.

distributed by several websites (GRACE Tellus; CU, Boulder; ICGEM).

In this study, 158 months of Release-05, Level-2 GRACE solutions have been used from the three official processing centers (RL05 in case of CSR and JPL, RL05a in case of GFZ) from the 95th day of 2002 to the 6th day of 2017. Determining each solution requires approximately a month of GRACE measurements. At least 28 observed days have been used in 129, 130 and 112 solutions, respectively for CSR, GFZ and JPL. Out of the remaining 29, 28 and 46 solutions there are 5, 4 and 9 cases respectively, when the number of the used days is less than 21. Due to the nearly meridional range rate observations, Release-05 (RL05 and RL05a) GSM products are uncertain for the C20, which, according to the recommendations, was replaced by SLR-derived C20 harmonics from GRACE Technical Note 07 (Dahle et al., 2012).

A $1^\circ \times 1^\circ$ grid has been created in order to study the total area of the Earth's surface. Surface mass anomaly time series have been calculated at each grid point based on Swenson and Wahr (2002). The CSR, GFZ and JPL spherical harmonic coefficients have been truncated at a maximum degree and order 60. To reduce the remaining short-wavelength errors of the GRACE solutions, a de-stripping filter has been applied according to Swenson and Wahr (2006) and the coefficients have been smoothed with a 300 km Gaussian filter (Jekeli, 1981). The surface mass anomalies have been expressed in terms of changes in equivalent water thickness, where a water thickness change of 1 mm corresponds to mass change of 1 kg/m^2 .

4. RESULTS

Based on these calculations, probable regions of multiannual variations have been detected. The

criteria of significant multiannual variation are defined as variations with at least 60 % of the annual signal in the 0.15 to 0.4 1/year frequency band. This criterion was defined by visual screening.

The regions with probable multi-annual mass variations are summarized in Figure 1. Each row shows the results achieved with the different GRACE data sets, while the columns represent the PSD estimation methods described above.

Performing exactly the same calculation on the different GRACE spherical harmonics leads to slightly different results. Minor dissimilarities appear along the outlines of the identified areas as a consequence of the choice of the input data. The arbitrariness of detecting grid points which show a significant periodic component with 3-7 years of period also influences the results. Still, the detected regions are pretty much the same, apart from an East-Antarctic area, where the JPL time series solely show clear multi-annual signal. Figure 2a shows the mass anomaly time series of a typical grid point from the investigated region. There are visible differences between the time series, and the correlations between them are remarkably low, especially compared with the results of the other regions. The GFZ time series represent minimal periodic behaviour, while CSR results show slightly clearer annual cycle. In comparison, JPL mass anomalies are dominated by a visible periodic component with an approximately 7-year cycle.

The results of the PSD estimations with the method of Welch are shown in Figure 2b. Similar results have been achieved with the Lomb-Scargle's and Thomson's methods as well: the CSR and GFZ time series represent minimal periodicity while the JPL mass anomalies show a noticeable annual cycle and a significant multi-annual cycle with a period of 6-7.5 years.

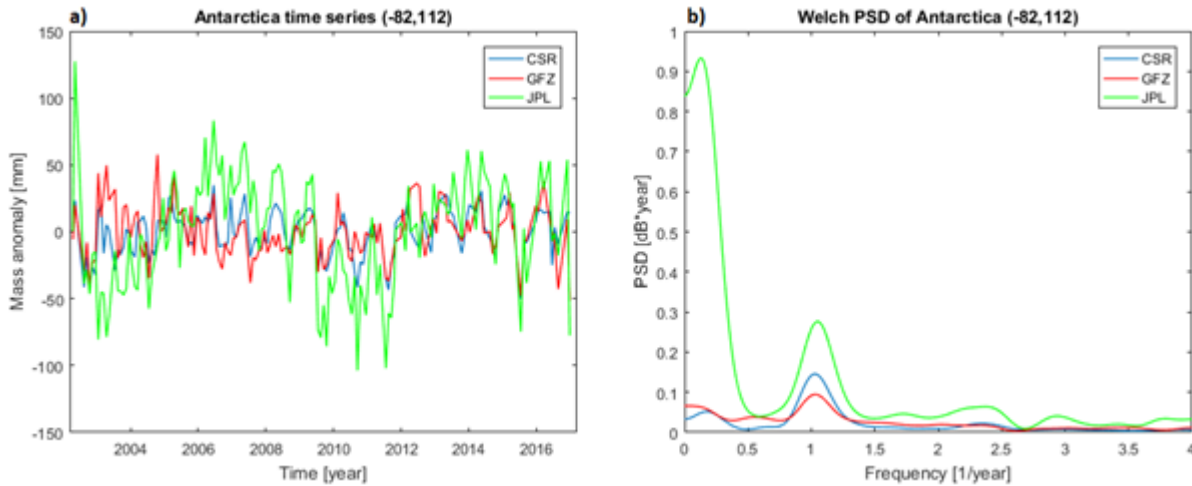


Fig. 2 a) Mass anomaly time series and b) Welch PSD estimations of Antarctica.

Table 1 Size of the areas with multi-annual periodic variations.

	Lomb-Scargle	Thomson	Welch	Σ
CSR	1099	1932	1219	522
GFZ	1131	2158	1271	528
JPL	1162	2386	1334	593
Σ	812	1318	895	372

Table 1 summarizes the results of each combination, where the number of grid points with multi-annual behaviour is used to describe the size of the regions. Based on the numbers, working with JPL and CSR data leads to the largest and smallest areas, respectively, while the GFZ results are repeatedly between them. However, if we subtract the above-mentioned East-Antarctic areas from the JPL results, the sizes of the remaining regions decrease below the CSR and GFZ results with the Lomb-Scargle and Welch calculations. Estimating PSD with the methods of Lomb-Scargle and Welch while using the same requirements to select the grid points with multi-annual variations leads to similar results with minor differences. The sizes of the Welch areas are 11 %, 12 % and 15 % larger than the Lomb-Scargle areas for the CSR, GFZ and JPL data, respectively; on the other hand, the 74 %, 72 % and 70 % of the Lomb-Scargle grid points are from the same areas, while in case of Welch's method, the overlapping areas contain the 73 %, 70 % and 67 % of the CSR, GFZ and JPL areas, respectively. Based on Figure 1 and Table 1, the multitaper method of Thomson leads to visibly different results. The contours of the regions with Thomson's multitaper method resemble the Welch areas, although the number of Thomson grid points are 158 %, 170 % and 179 % higher (comparisons with the Lomb results give 176 %, 191 % and 205 %), for the CSR, GFZ and JPL time series, respectively. 68 % of the CSR, 61 % of the GFZ and 55 % of the JPL grid points are from the same regions with the multitaper estimation. These values suggest that searching significant multi-annual signals from slightly different datasets with Thomson's method leads to results with higher discrepancy; there are

more differences between the selected areas compared to the other two methods. Combining all datasets and all methods, the total number of mutual grid points is 372. Excluding one of the GRACE spherical harmonics sets does not lead to significant development. On the other hand, the similarity between the Thomson and Welch results is conspicuous: eliminating the Lomb-Scargle method nearly doubles the size of the total overlapping areas (702 points). Figure 3a represents the overlapping regions of significant periodic variations with a period between 3 and 7 years based on all the GRACE datasets and the Lomb-Scargle periodogram, while Figure 3b shows the combination of the results from the methods of Thomson and Welch. Figure 3c summarizes all the results and shows the mutual significant regions from Figures 3a and 3b. In case of the grid points which are not included in the final 372 but appear either on Figure 3a or 3b, typically all the PSD estimations indicate a multi-annual component, however with a lower magnitude. The further investigations of this study are limited to the 8 following regions with significant multi-annual periodic mass variations: Canada, United States, Argentina, Romania, Democratic Republic of Congo, Russia, Tajikistan and Australia.

5. ANALYSIS OF MULTI-ANNUAL MASS VARIATIONS

Eight grid points have been specified to investigate the multi-annual mass variations of the above-mentioned regions. Due to the noticeable similarity of the different GRACE time series, only the CSR mass anomalies and the corresponding PSD estimations are represented in Figure 4. The

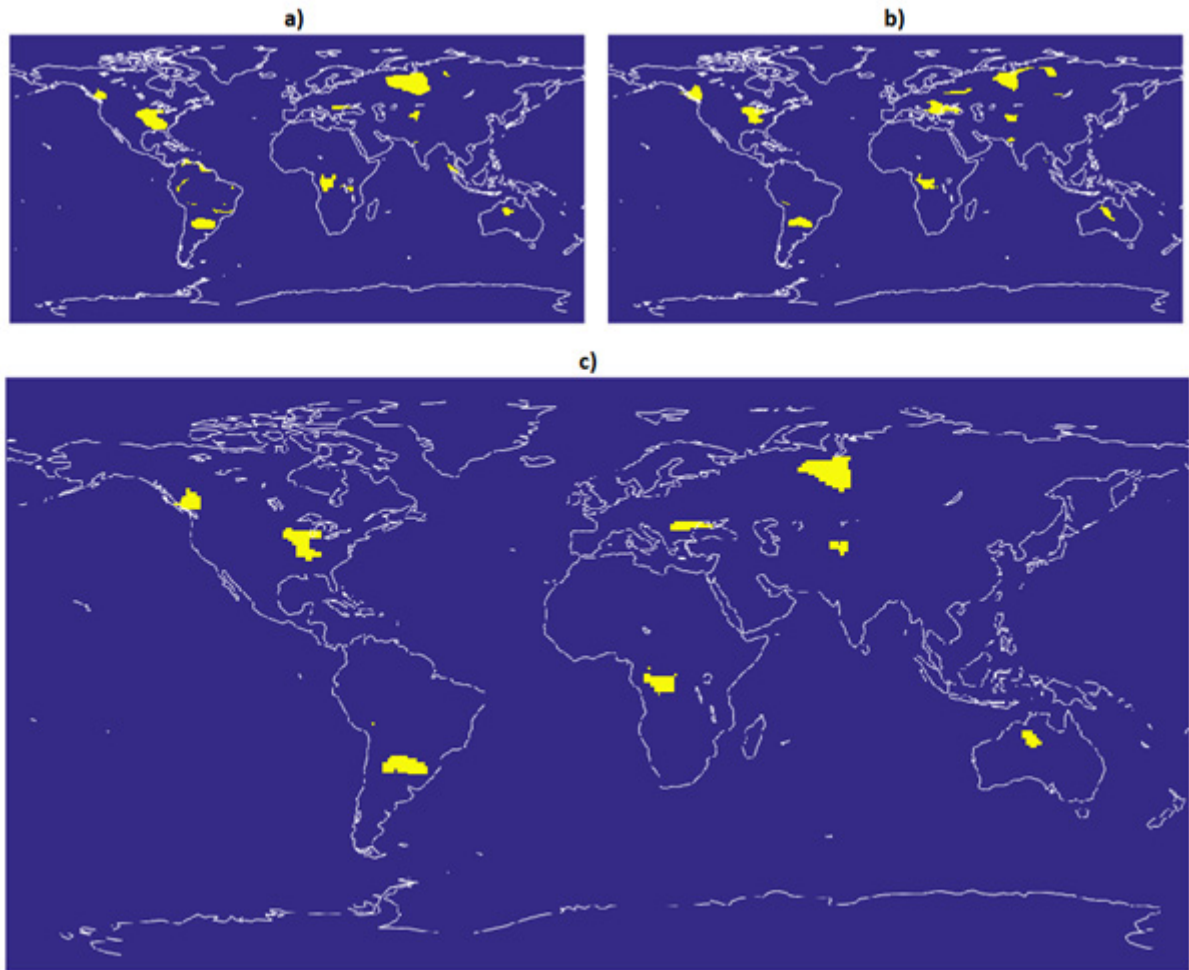


Fig. 3 Summarized results a) with the method of Lomb-Scargle, b) with the combination of the methods of Thomson and Welch and c) the final results.

characteristics of the PSD estimation methods are conspicuous. The method of Welch leads to the smoothest results with definite maxima, the graph from the multitaper of Thomson varies rapidly and has multiple peaks, while the oscillating Lomb-Scargle periodogram has the highest frequency resolution. Despite their differences, all methods give similar PSD estimations, although the identification of the dominant frequencies corresponding to the variations with a period between 3 and 7 years is uncertain, especially with Thomson's multitaper. The typical annual hydrologic mass variations are dominant in Canada, Romania, DR Congo, Russia and Tajikistan; weaker annual signals appear in the US and Australia, while the mass variations in Argentina do not represent any seasonality. In case of the African test point, a strong half-year periodic component occurs due to the location of the area: there are 2 wet seasons near the Equator. In fact, the mass variation time series of DR Congo reflect the precipitation patterns with only a few months of delay. In the other investigated regions, the rainfall patterns are not as homogenous as in the tropics, thus precipitation time series in the grid point coordinates do not resemble the water mass variations of the area. Global rainfall time series used in this study for comparison were downloaded from the webpage of the Joint

Research Centre of the European Commission (Ziese et al., 2011).

According to the discussion before, multi-annual water mass variations may be associated with the ENSO cycle. During the El Nino and La Nina events, the Sea Surface Temperatures (SST) of the Pacific Ocean deviated from the normal values. Figure 5 shows the Oceanic Nino Index (ONI) time series for our investigated period from the ERSSTv5 model (Huang et al., 2017). The used values are the running 3-month mean SST anomalies for the Nino 3.4 region (5°N-5°S, 120°-170°W). Weak/moderate/strong/very strong El Nino events are defined by at least 0.5/1/1.5/2 anomalies (i.e. warmer sea surface) and can lead to extreme weather conditions globally. The -0.5/-1/-1.5 values (i.e. below average sea surface) suggest weak/moderate and strong La Nina periods with opposite effects. In the present study we focus on the ENSO events with effect on the rainfall variations of our investigated regions.

Most of the ENSO events have an impact on the weather conditions of the Canadian, Argentinian and Australian areas from Figure 3c.

In Canada, the province of British Columbia receives above average rainfall during La Nina, while El Nino brings warmer and drier conditions. The mass variations from GRACE in British Columbia are

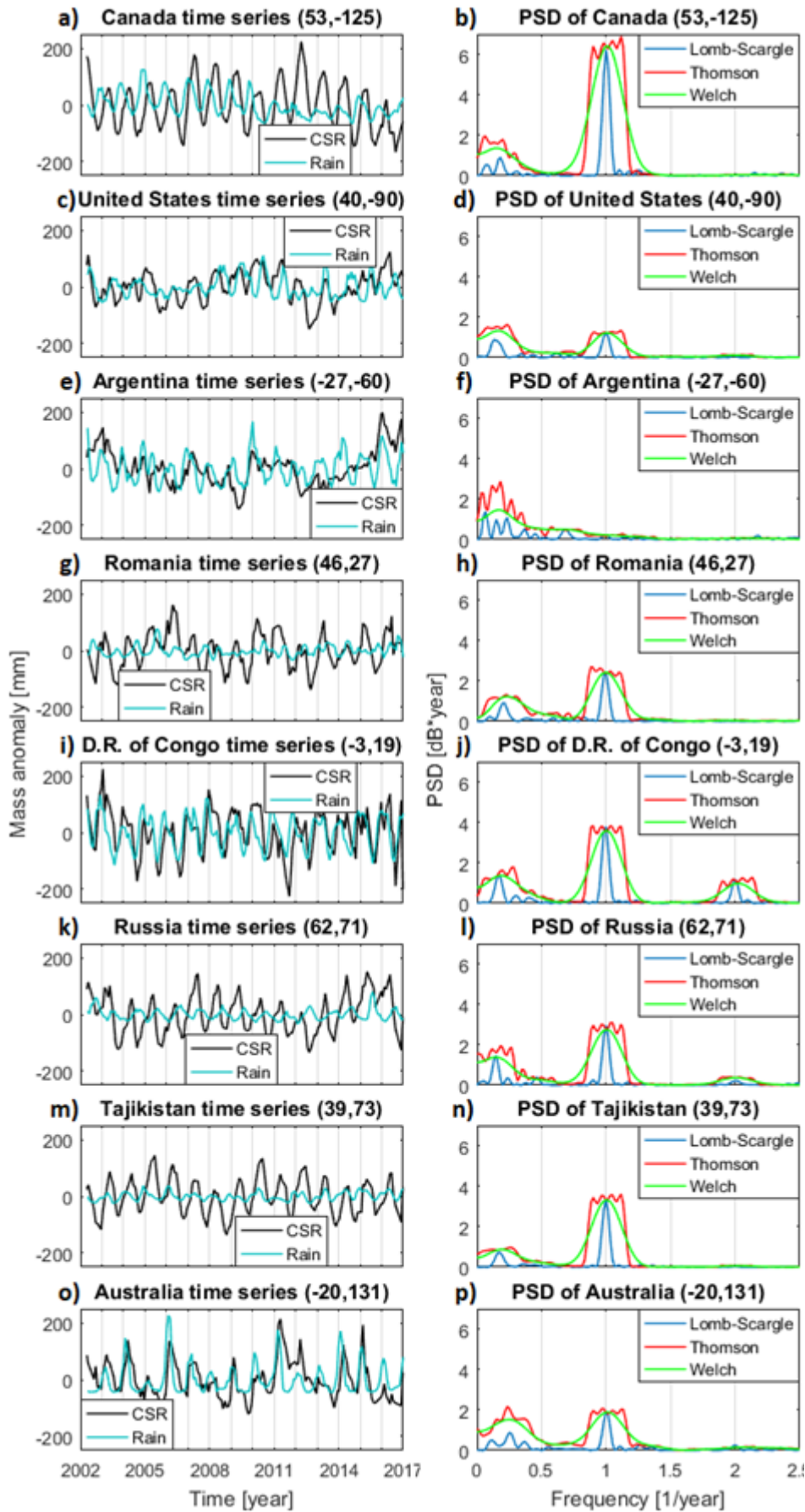


Fig. 4 Mass anomaly with rainfall time series and PSD estimation results of the investigated regions.

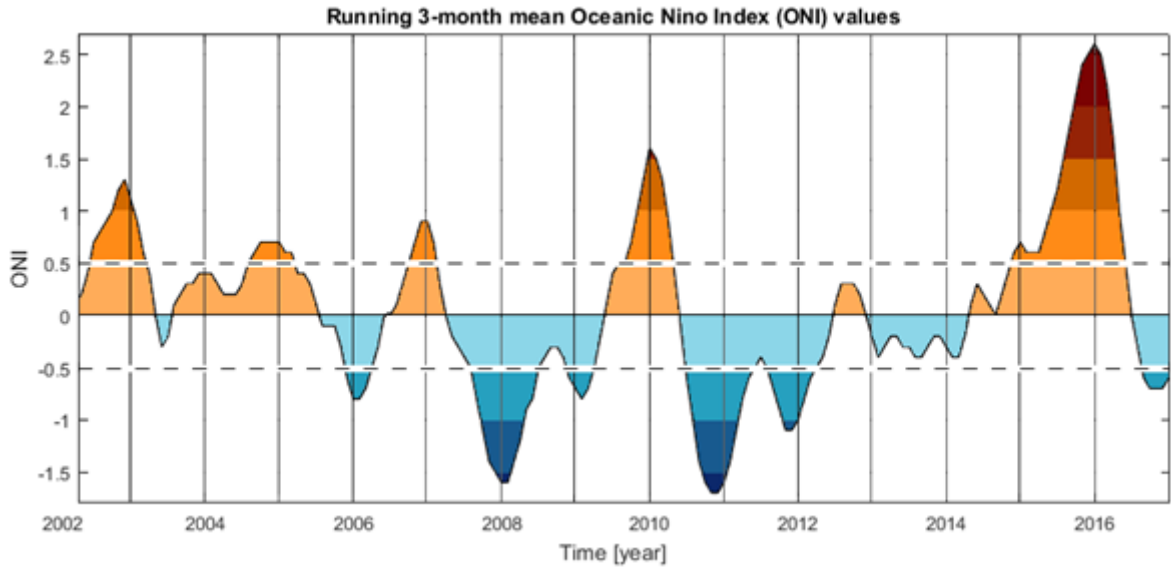


Fig. 5 ONI time series between 2002 and 2017. The higher positive (negative) values indicate the stronger El Nino (La Nina) events.

shown in Figure 4a. The El Niño in 2002-03, 2009-10 and 2015-16 can be responsible for the decrease in 2002, the lower peak in the beginning of 2010, and the negative trend during 2015 and 2016. The moderate and strong La Niña events in 2007-08 and 2010-11 are reflected in Figure 4a as positive trends. According to the Canadian Drought Monitor, during the second half of 2006, 2009-10, and 2013-14-15, moderate or worse droughts struck our investigated region. The PSD estimations show the most dominant annual variations in Canada and a 5-6.5-year multi-annual cycle, which are confirmed by these weather conditions and the time series as well.

The time series and PSD estimations of Argentina clearly differ from the other results. The absence of the annual mass variations despite of the seasonality of the rainfall patterns can be originated in complex hydrologic processes. In one of our previous study, we have found that the lack of seasonal water mass variations is typical in the most of the La Plata basin due to the presence of massive dams, waterfalls and the Guarani aquifer (Kiss and Földvály, 2017). The ENSO events have the opposite effect compared to Canada. The El Niño periods in 2002, 2006-07, 2009-10 and 2015-16 are responsible for the increasing mass anomalies, while the La Niña events are followed by the lowest mass anomalies in 2009 and 2012. In fact, the time series showed in Figures 4e and 5 both reveal and longer periodic variation; a negative trend followed by a peak around 2010, and a definite increase until the end of 2015.

In the Northern Territory of Australia, the majority of the annual precipitation occurs during the wet season which coincides with the typical El Niño months, thus El Niño can lead to extreme droughts. In all cases when the ONI reaches 0.5, the maxima in the beginning of each year are below the usual value (Fig. 4o). During the weak La Niña at the beginning of 2006, record rainfall was registered near the investigated area. On the other hand, the effect of the stronger 2007-08 La Niña is not obvious: the mass

anomalies only show the mass gain at the end of 2008, however 2007 and 2008 were the driest years between 2002 and 2017. The effect of the strong 2010-11 La Niña event is reflected in Figure 4o. The peak at the beginning of 2011 can be connected to the Tropical Cyclone Carlos, which brought a monthly precipitation on 16-17 February. Besides these ENSO-driven cases, extreme rainfall occurred during the February of 2004 and in the first months of 2014 and 2015, causing local maxima in the mass anomaly time series. Figure 4p indicates an annual and a 4-year period multi-annual mass variation with all the estimation methods.

The American grid point is located in Illinois where the ENSO events have no clear effect. Comparison between Figure 4c and Figure 5 does not show any correlation either. According to the US Drought Monitor and precipitation time series, dry (2005-07 and 2011-12) and wet (2008-10 and 2014-16) periods follow each other, which is in accordance with the multi-annual variations with a period of 6-7 years based on the PSD estimations. In addition, the historical Illinois River water level crests provided by NOAA on its National Weather Service website (NOAA, 2017) coincide with the peaks of the time series: 2002.05., 2005.01., 2008.09., 2009.03. and 05., 2010.06., 2013.04., 2015.07. and 2016.01.

The effect of the ENSO events is minimal in the test regions of Romania, DR Congo, Russia and Tajikistan. Except for the grid point in Tajikistan which is located in the Pamir Mountains, all the regions are parts of great river basins: the Danube, the Congo and the Ob basins. The GRACE time series are in a few months of delay compared to the precipitation data in Congo and Tajikistan. In the Danube and Ob basins, the precipitation time series and the mass anomalies of the investigated grid points are out of phase. The periods of the observed multi-annual variations (Romania: 4-5 years, DR Congo: 5-6 years, Russia: 5.5-7 years, Tajikistan: 4-6 years) are not connected directly to the ENSO cycle, although, it is

possible that they are consequences of simultaneous ENSO, other regional phenomena (e.g. North Atlantic Oscillation) and local weather anomalies.

6. DISCUSSION

The surface mass anomaly time series based on the monthly spherical harmonics from the measurements of the GRACE satellites have been used to study multi-annual mass variations between 2002 and 2017 on a global level. Note that there have been very few attempts to determine multi-annual mass variations so far. Ramilien et al. (2014) made a Principal Component Analysis for 9 year-long GRACE mass anomaly time series, after performing a kind of low-pass filtering with a 13-month moving window. According to their results, they have detected a relevant mass loss in the Congo basin for the period of 2003–2012, which is overwhelmed by the mass gain processes in the neighbouring Zambezi, Niger and Volta basins. Methodologically, beyond the description of the long-term mass loss or gain process, Ramilien et al. (2014) has not determined the frequency of the multi-annual phenomenon.

In this study three different PSD estimation methods have been applied to identify the regions of mass variations with a period between 3 and 7 years. As a result, eight different areas have been found with significant multi-annual mass variations: British Columbia (Canada), Illinois (US), Province of Chaco (Argentina), Eastern Romania, Western DR Congo, West Siberia (Russia), Tajikistan and the Northern Territory of Australia. Except for British Columbia and Tajikistan, where there is probability of ice mass movements due to the glaciers, the main mass variations are typically water mass changes. Multi-annual periodic water mass variations are often connected to the ENSO events, although, the alternation of the El Niño and La Niña phases is not periodic. In our case, ENSO effects can be observed in the time series of Canada, Argentina and Australia. In other regions, the influence of the ENSO events is not clearly detectable. In summary, the discovered multi-annual mass variations for the investigated period differ in period and phase as well, and they are results of simultaneous local and global weather anomalies.

Note finally, that the correlation of the derived multi-annual variations of mass with the ENSO events may be theoretically a difficulty. According to Privalsky (2015), relationships between time series studied on the basis of cross-correlation coefficients and regression equations may result in incomplete or erroneous conclusion. Instead, multivariate linear autoregressive methods (Box et al., 1994; Kashyap and Rao, 1976; Privalsky and Jensen, 1995; Privalsky, 2015) seem to provide more reliable comparison. Comparison of the multi-annual variations of the ENSO and of the mass variations by an appropriate method should be the next step of the present research.

REFERENCES

- Box, G.E.P., Jenkins, G.M. and Reinsel, G.C.: 1994, *Time Series Analysis. Forecasting and Control*, 3rd edition, Prentice-Hall, Englewood Cliffs, NJ, 598 pp.
- Huang, B., Thorne, P.W., Banzon, V.F., Boyer, T., Chepurin, G., Lawrimore, J.H., Menne, M.J., Smith, T.M., Vose, R.S. and Zhang, H.M.: 2017, Extended reconstructed sea surface temperature version 5 (ERSSTv5): Upgrades, validations, and intercomparisons. *J. Climate*, 30, 20, 8179–8205. DOI: 10.1175/JCLI-D-16-0836.1
- Jekeli, C.: 1981, Alternative methods to smooth the Earth's gravity field. OSU Report Series, 327, 48 pp.
- JPL: 2018, GRACE Tellus publications, link: <https://grace.jpl.nasa.gov/publications/> (last access on 27 May 2018).
- Kashyap, R. and Rao, A.: 1976, *Dynamic Stochastic Models from Empirical Data*. Academic Press, New York, 334 pp.
- Kiss, A. and Földváry, L.: 2017, Seasonal hydrologic variations in the La Plata basin from GRACE gravity field models. *Acta Geodyn. Geomater.*, 14, 2, 145–152. DOI: 10.13168/AGG.2016.0035
- Lomb, N. R.: 1976, Least-squares frequency analysis of unequally spaced data. *Ap&SS*, 39, 2, 447–462. DOI: 10.1007/BF00648343
- NOAA: 2018, Historical Illinois River water level crests. National Weather Service website, link: https://water.weather.gov/ahps2/crests.php?wfo=ilx&age=havi2&crest_type=historic (last access on 27 May, 2018).
- Privalsky, V. and Jensen, D.: 1995, Assessment of the influence of ENSO on annual global air temperature. *Dynam. Atmos. Oceans*, 22, 161–178.
- Privalsky, V.: 2015, On studying relations between time series in climatology. *Earth Syst. Dynam.*, 6, 1, 389–397. DOI 10.5194/esd-6-389-2015
- Ramillien, G., Frappart, F and Seoane, L: 2014, Application of the regional water mass variations from GRACE satellite gravimetry to large-scale water management in Africa. *Remote Sens.*, 6, 8, 7379–7405. DOI: 10.3390/rs6087379
- Scargle, J. D.: 1982, Studies in astronomical time series analysis. II - Statistical aspects of spectral analysis of unevenly spaced data. *ApJ*, Part I, 263, 835–853. DOI: 10.1086/160554
- Swenson, S. and Wahr, J.: 2002, Methods for inferring regional surface-mass anomalies from Gravity Recovery and Climate Experiment (GRACE) measurements of time-variable gravity. *J. Geophys. Res., Solid Earth*, 107, B9. DOI: 10.1029/2001JB000576
- Swenson, S. and Wahr, J.: 2006, Post-processing removal of correlated errors in GRACE data. *Geophys. Res. Lett.*, 33, L08402. DOI: 10.1029/2005GL025285
- Tapley, B.D., Bettadpur, S., Watkins, M. and Reigber, C.: 2004, The gravity recovery and climate experiment: mission overview and early results. *Geophys. Res. Lett.*, 31, 9, L09607. DOI: 10.1029/2004GL019920
- Thomson, D. J.: 1982, Spectrum estimation and harmonic analysis. *Proc. of the IEEE*, 70, 9, 1055–1096. DOI: 10.1109/PROC.1982.12433
- Welch, P. D.: 1967, The use of fast Fourier transform for the estimation of power spectra: A method based on time averaging over short, modified periodograms. *IEEE Trans. on Audio and Electroacoustics*, 15, 2, 70–73. DOI: 10.1109/TAU.1967.1161901
- Ziese, M., Becker, A., Finger, P., Meyer-Christoffer, A., Rudolf, B. and Schneider, U.: 2011, GPCC First Guess Product at 1.0°: Near Real-Time First Guess monthly Land-Surface Precipitation from Rain-Gauges based on SYNOP Data. DOI: 10.5676/DWD_GPCC/FG_M_100